POWER OSCILLATION DAMPING FOR CONTROL OF PMSG BASED WIND TURBINE SYSTEM FOR INERTIAL RESPONSE

[1]G.LAVANYA KUMARI,
M.Tech, Dept.of EEE, JNTUA,Anantapuramu,A.P

Abstract: ***An improved active power control method for variable speed wind turbine to enhance the inertial response and damping capability during transient events, by using the optimized power point tracking (OPPT) inertia control (VIC) curves according to the frequency deviation, is proposed to release the "hidden" kinetic energy and provide controller, which shifts the turbine operating point from the maximum power point tracking (MPPT) curve to the virtual dynamic frequency support to the grid. The effects of the VIC on power oscillation damping capability are theoretically evaluated. Thus, inertial response and power oscillation damping function can be obtained in a single controller by the proposed OPPT control. The model of wind conversion system is built and simulated along with PI controller and fuzzy controller to reduce oscillations and increase the active power by using MATLAB/SIMULINK software is developed.***

Index Terms—Frequency support, permanent magnet synchronous generator (PMSG), power oscillation damping, variable speed wind turbine, virtual inertia control (VIC).

1 .INTRODUCTION

In these days two types of generator used in large scale WECS for convert the wind power into electrical power which are doubly fed induction generator (DFIG) and Permanent magnet synchronous generator (PMSG). PMSG is a Direct Drive type generator; and don't require gear box and excitation current so PMSG show good performance. WECS with PMSG can avoid the problem of wear and tear of gear, it can help wind turbine operate more reliable and reduce maintenance. WECS can be used in two different ways namely isolated standalone system and Grid connected system. Standalone systems are employed to the needs of small scale industries for rulers areas, such system are located at for off places/remote areas. Grid connected system increased energy efficiency, robustness, voltage support, diversification of energy sources, reduced transmission and distribution losses and reliability of the system. This paper described the model and simulation of PMSG based on WECS in d-q model.

In recent years, the reduced inertial response and power damping capability, as the result of increased wind power penetration in ac networks, have been receiving considerable attention from wind turbine manufactures and system operators. Tackling these issues requires not only fault ride through capability of the wind turbines, but also the ability to participate in frequency and power regulation during system disturbances so as to make the wind farms grid-friendly power generation sources. Thus, the control potential of variable speed wind turbines need be further explored to ensure the stability of power networks containing large-scale wind energy. Traditional synchronous generators naturally contribute to inertial response with their inherent inertia during frequency events. However, variable speed wind turbines do not directly contribute to system inertia due to the decoupled control between the mechanical and electrical systems, thus preventing the generators from responding to system frequency changes. In addition, the power system stabilizer (PSS) is normally equipped in the traditional synchronous generators to provide power damping during and after large disturbances. With increased wind penetration, it also becomes essential for wind turbines to provide power oscillation damping. This can be critical for weak power systems containing large scale wind farms, as damping from synchronous generators may be insufficient and active contribution from wind farms becomes essential.

At present, auxiliary controllers with frequency feedback are introduced to wind turbines to provide system frequency response, such as P/f droop controller, PD controller, and reloading controller by shifting the maximum power point tracking (MPPT) curves. However, the P/f droop controller equipped in the blade pitch control system can only emulate the primary frequency response. While the PD controller of the converter employs a df/dt term to emulate additional inertia in the initial frequency change period and the power tracking curve is shifted from the MPPT curve to the right suboptimal curve to provide dynamic frequency support for the grid during a frequency event. However, a smooth recovery to the MPPT operation cannot be realized by these control approaches. Moreover, the damping capabilities of these controllers during grid disturbance are not analyzed. The traditional PSS has been introduced to the DFIG to damp power system oscillations but no frequency support was considered. For all the work reported, simultaneous inertia and damping control cannot be achieved.

II.MATHEMATICAL MODEL

This section will present mathematical model of PMSG base on WECS. It consists of wind energy conversion, wind turbine, drive train, PMSG and converter as show in Fig. 1.

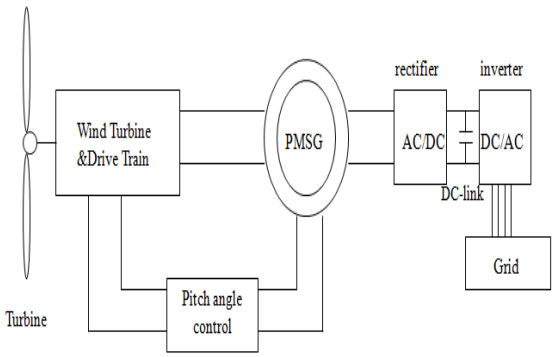

Fig.1. PMSG based on WECS

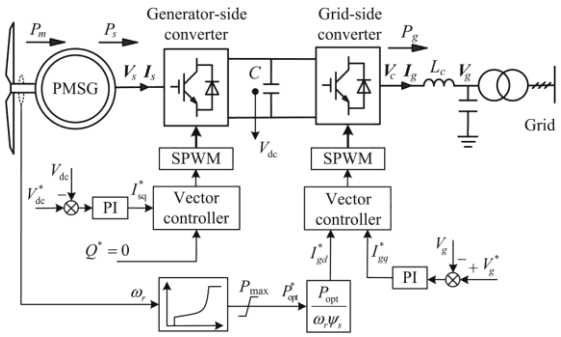

Fig.2.Schematic control diagram of a PMSG-based wind turbine

A. Wind Energy Conversion

The kinetic energy of wind is given by,

$E_c=\frac{1}{2}mv^2$ (1)

m= ρvS (2)

m = air mass

v = wind speed

ρ = air density

S = covered surface of the turbine.

The wind power is given by,

$P_w = E_c = \frac{1}{2}mv^2 = \frac{1}{2}\rho S v^3$ (3)

B. Wind turbine

Wind turbine is applied to convert the wind Energy to mechanical torque. The mechanical torque of turbine can be calculated from mechanical power at the turbine extracted from wind power. This fact of the wind speed after the turbine isn't zero. Then, the power coefficient of the turbine(C_p)isused. The power coefficient is function of pitch angle (β) and tip speed (λ), pitch angle is angle of turbine blade whereas tip speed is the ratio of rotational speed and wind speed. The power coefficient maximum of (C_p) is known as the limit of The power coefficient is given by,

$$C_p(\lambda,\beta) = C_1\left(\frac{C_2}{\lambda_i} - C_3\beta - C_4\right)e^{-c_5} + C_6\lambda \quad (4)$$

where, P_m = the mechanical output power of the turbine C_p = the performance coefficient of the turbine ρ = the air density

S = the turbine swept area

V_{wind}= the wind speed

k_p = gain power

λ = the tip speed ratio

β = the blade pitch angle

The mechanical torque is given by

$T = P_m/\omega$

III.CONTROL OF PMSG

The proposed inertia and damping control methods are developed considering the power regulation of PMSG-based wind turbine. The dynamic model of the PMSG and associated converters can be found.

The electromagnetic power of the generator can be controlled using either the generator-side converter or the grid-side converter. In this paper, the grid-side converter directly controls the generated active power, where as the generator-side converter is used to maintain a constant dc-link voltage, as seen in Fig. 1. Since the grid-side converter can fall into current limit during ac voltage dip with reduced power transmission, the generator- side converter as the dc voltage control station automatically reduces power generation in order to maintain a constant dc voltage. This control scheme provides automatic power balance during ac fault and simplifies fault ride through control of the PMSG. The surplus power in the turbine during such disturbances is stored as the kinetic energy of the large rotating masses but only results in a relatively small speed fluctuation of the PMSG. If required, the acceleration of generator speed can be limited using the pitch control to prevent it from going above its rated value.

Under normal operation, the generated power of the wind turbine is controlled under the MPPT according to its rotor speed, and is grid frequency due to the fast converter control .the reactive power of PMSG control to zero or to be regulated to maintain a stator voltage minimize the power loss of the generator. to emu late the dynamic response of synchronous generators using PMSG-based wind turbines, advanced control schemes considering grid frequency deviation need be added to the grid-side converter's power control loops. Thus, the rotor speed of the PMSGs is regulated to release/store the kinetic energy to make the "hidden inertia" available to the connected grid, and its flexible power control can also be utilized to participate in power system oscillation damping.

It needs to be noted that the ability for a wind turbine to pro- vide inertia support and damping is based on the condition that the wind turbine and associated generator and converter system have the spare power capability. This means that prior to the network disturbance, the wind turbine is operating at below- rated power, which is usually the case, as wind turbines are usually only partially loaded.

IV.VIRTUAL INERTIA CONTROL OF VARIABLE SPEED WIND TURBINES

A. Principle of Virtual Inertia Control(VIC):

The inertia constant H_{tot} of a power system with synchronous generators and variable speed wind turbines can be expressed as,

$$H_{tot} = \left[\frac{(\sum_{i=0}^{m}(J_{s_i i}\omega_e^2)}{2p_{s_i}^2}\right] + \sum_{j=1}^{n} E_{\omega\_j}/S_N \quad (5)$$

Where m and n are the numbers of connected synchronous generators and wind turbines in the grid, respectively .p_{s_i} and J_{s_i} are the numbers of pole pairs and moment of inertia for synchronous generator i, respectively. E_w is the effective kinetic energy of the wind turbine available to the power system. S_N is the total nominal generation capacity of the power system.

As the stored kinetic energy in variable speed wind turbines cannot be automatically utilized during frequency changes as that of conventional synchronous generators [i.e., E_w= 0 in replacing conventional plants with large numbers of variable speed wind turbines under MPPT control can significantly reduce the effective inertia of the whole system. In addition, if newly installed wind farms are added to the power system without changing the conventional plants, S_N is increased but the total kinetic energy available to the power system remains unchanged. In this case, the effective inertia of the whole system is also reduced. This can have significant implications for power system operation and could lead to large frequency deviation. Therefore, it is important to make full use of the stored energy in the wind turbines. To better describe kinetic energy in wind turbines' rotating masses, the definition of the virtual inertia of variable speed wind turbines is given first.

The mechanical characteristics of a wind turbine generator can be expressed as,

$$P_m - P_e = J_\omega \omega_r \frac{d\omega_r}{P_\omega^2 dt} = \frac{J_\omega \omega_r d\omega_r}{\omega_s d\omega_s} \times \frac{\omega_s d\omega_s}{P_\omega^2 dt} = J_{vir}\omega_s \frac{d\omega_s}{P_\omega^2 dt}$$
$$J_{vir} = J_\omega \omega_r d\omega_r / (\omega_s d\omega_s) \quad (6)$$

Where ω_r is the rotor electrical angular speed and p_w is the number of pole pairs of the wind turbine generator. P_m and P_e are the mechanical and electromagnetic powers of the wind turbine, respectively. J_w is the combined natural inertia of the wind turbine system. J_{vir} is defined as the virtual inertia of the wind turbines.

If the wind turbine is controlled to provide dynamic support using its kinetic energy during a frequency change, the released kinetic energy ΔE_k can be obtained from (2)as

$$\Delta E_\omega = \int (P_m - P_e) dt = \int \left(\frac{J_{vir}\omega_s}{P_\omega^2}\right) d\omega_s \quad (7)$$

If the converter controls J_{vir} to be constant by adjusting the rotor speed and to move away from the MPPT point, the effective kinetic energy of the wind turbine compared with a synchronous generator can be expressed as

$$E_\omega = (\tfrac{1}{2}) J_{vir} (\tfrac{\omega_e}{P_\omega})^2 \quad (8)$$

Where $\Delta\omega_s$ and $\Delta\omega_r$ are the changes of the grid and rotor angular speed during a frequency event ,respectively ,λ is defined as the virtual inertia coefficient, and ω_{r0} is the pre disturbance rotor speed.

It can be observed from (6) that the virtual inertia of the wind turbine is determined not only by its natural inertia, but also by the pre disturbance rotor speed ω_{r0} and the virtual inertia coefficient λ. Different to synchronous generators, whose rotor speeds are coupled directly to the system frequency, i.e., λ = 1, the speed variation of the variable speed wind turbine can be much greater than the system frequency variation due to the asynchronous operation, i.e., $\Delta\omega_r > \Delta\omega_e$ and thus $\lambda > 1$. Therefore, the virtual inertia of the PMSG-based wind turbine can be several times of its natural inertia. However, the stored energy in the wind turbine changes with its rotor speed and is dependent on the wind velocity. Thus, the available virtual inertia also depends on the pre disturbance rotor speed of the wind turbine.

B. Supplementary Derivative Control:

The generated power of PMSG control can be controlled according to the grid frequency deviation to emulate inertial response. The auxiliary power reference P_f^* can be derived from (2) as

$$P_m - P_e = P_M - (p_{opt}^* - P_f^*) \sim P_f^*$$
$$= J_{vir}(\tfrac{\omega_s d\omega_s}{P_\omega^2 dt}) \quad (9)$$

Fig. 3. Block diagram of wind turbine inertia response.

Thus, the virtual inertia can be emulated using a supplementary control loop in addition to the normal MPPT controller.

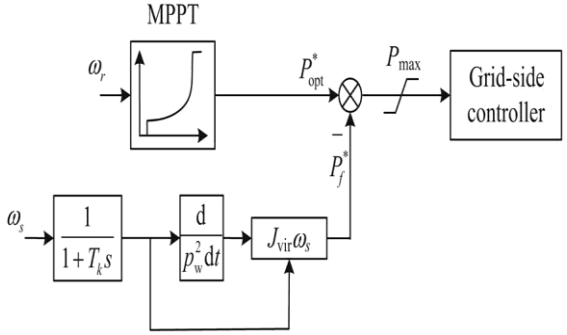

Fig. 2.shows the principles of such wind turbine inertia response for system frequency support, and similar schemes have also been investigated in previous research and tested in variable wind turbine.

C.OPPT control for the inertial response:

In order to achieve better inertia response, the above- described interaction between the supplementary inertia control and the MPPT control must be avoided. The VIC proposed in this paper is based on the optimized power point tracking (OPPT) method. When system frequency deviation is detected, the generated power is regulated rapidly by switching the turbine operating point from the MPPT curve to the defined VIC curves. By this way, the kinetic energy in the wind turbines can be fully utilized to emulate the inertia response.

The generated power based on the conventional MPPT control can be expressed as

$$P_{opt}^* = \{\frac{K_{opt}\omega_r^3, (P_{max} - K_{opt}\omega_1^3)}{(\omega_{max} - \omega_1) + P_{max}(\omega_1 < \omega_r < \omega_{max}), P_{max}} (\omega_r - \omega_{max})$$
(10)

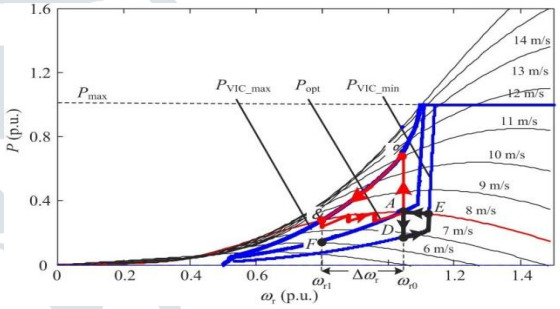

Fig. 4. Scheme of the VIC-based power point tracking curve.

$P\omega$ is used for the constant speed stage, and ω_1 is the initial angular speed in this stage. P_{max} is the maximum active power output of the PMSG.

From(8), It can be observed that different curve coefficients will generate a series of power tracking curves, defined as VIC curves. Thus, the regulation of the PMSG's operation point can be achieved by moving it from the MPPT curve with coefficient k_{opt} to the VIC curve with coefficient k_{VIC}.

The principle of the OPPT control scheme for virtual inertial response is shown in Fig. 3. The wind velocity is assumed to remain constant at 8 m/s in this example. In reality, the wind speed could vary even during such a short period, which could affect the inertia support capability of the wind turbine. The impact of such wind speed variation on the effectiveness so the OPPT control will be further explored in future work. In the event of a system frequency drop, the wind turbine needs to decelerate to release the stored kinetic energy. Thus, the coefficient k_{opt} is increased and the power tracking curve is switched to the VIC curve. The operating point moves from the initial point A to B and then along the P_{VIC_max} curve to C. The rotor speed at point C (ω_{r1}) can be expressed using the frequency deviation as

$$\omega_{r1} = \omega_{r0} + \Delta\omega_r = \omega_{r0} + \lambda\Delta\omega_s$$
$$= \omega_{r0} + 2\pi\lambda\Delta f \quad (11)$$

If the wind speed remains constant, the captured active power at point A can be considered to be similar to that at point C for small rotor speed range. Thus, the VIC curve coefficient k_{VIC} can be calculated as

$$K_{VIC} = [\omega_{r0}^3/(\omega_{r0} + 2\pi\lambda\Delta f)]k_{opt} \quad (12)$$

According to (10), the VIC curve coefficient k_{VIC} is the function of the frequency deviation and replaces the constant coefficient k_{opt} of the MPPT curve. As illustrated in Fig. 3, in the event of a

frequency drop, the dynamic response of the VIC can be divided into two stages: 1) fast dynamic frequency support stage (A B C) and 2) slow rotor speed recovery stage (C A). Once the frequency decreases, k_{VIC} increases from the original value k_{opt} and rapidly reaches its upper limit during the first stage. According to(8)and(10),the corresponding power reference curve will then be shifted from P_{opt} to P_{vic_max} and the turbine's operating point is shifted from A to B with its output power changed from P_A to P_B. Since the generated power is greater than the captured mechanical power, the rotor decelerates and the operating point moves along the P_{vic_max} curve to the operating point C. Consequently, the kinetic energy stored in the rotating mass is released to support the grid frequency.

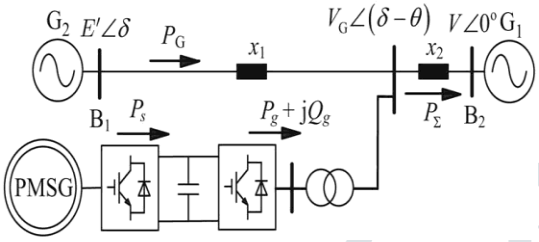

fig. 5.diagram of active power point tracking control.

V.IMPACT OF VIC ON POWER OSCILLATIONDAMPING

Normal variable speed wind turbines generate power in accordance with the wind speed and do not respond to grid disturbance such as power oscillations. Thus, networks having high wind penetration may experience higher oscillations after disturbance due to reduced system damping. However, if the VIC regulator is implemented in the wind turbines, the fluctuation of the generated active power as the result of inertia control can also affect power oscillation, which could lead to further reduction of system damping. Such potential risk on stable system operation with reduced power oscillation damping may prevent inertial control from being widely applied to wind turbines, even if an improved frequency performance can be achieved.

The equivalent circuit of a three-machine power system, as shown in Fig. 5, is used here for the theoretical evaluation of the effect on damping capability.

Fig. 6. Equivalent circuit of the power system with wind farms.

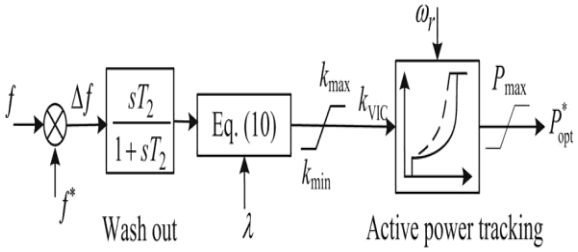

VI.SIMULATION DIAGRAMS

A. without VIC:

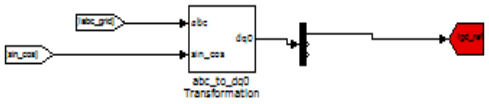

Fig.7.Simulation model of control of PMSG with VIC .

B.with VIC($\lambda = 1$):

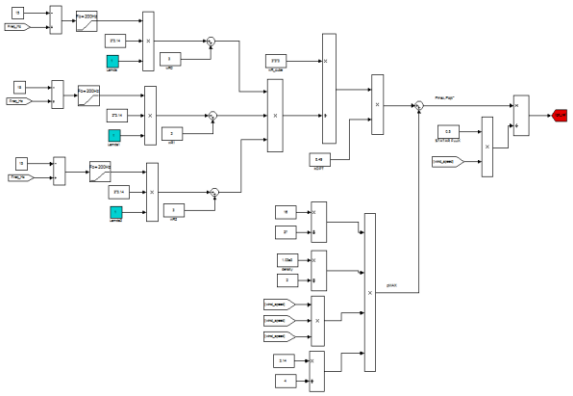

Fig.8.Simulation model of control of PMSG with VIC(λ =1) .

C. With VIC($\lambda = 9$):

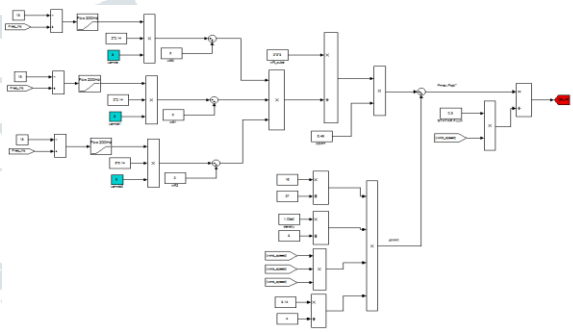

Fig.9.Simulation model of control of PMSG with VIC(λ =9) .

VII.SIMULATION RESULTS

It consists of two synchronous generators (G_1 and G_2), a PMSG-based wind turbine with the mechanical turbine and drive chain emulated using a controlled machine set, and three aggregated loads (L_1, L_2, and L_3). G_1 and G_2 are rated at 15 and 6.8 kVA, respectively. The wind turbine is rated at 10 which gives a wind power penetration level of around 31% for the tested system. The three loads L_1, L_2, and L_3 can be varied during tests and their maximum ratingsare10,4,and 4kW,respectively.

The sampling time of the control system is 50μs and the PWM frequency for the PMSG converters is 10 kHz. In the experiments, G_1 regulates frequency by its governor with 4% droop setting, whereas G_2 operates at constant active power mode and does not participate in frequency regulation.

A. Inertial Responses Under Sudden Load Change

The impact of different virtual inertia coefficients on the wind turbine inertia response and system frequency is tested first, and the results are shown in Figure. The wind velocity was setas8m/s by the motor-based emulator and the PMSG-based turbine initially operated at the maximum power point. During the test, Load L_1 was increased from 5.2 to 6.2 kW causing a temporary fall of the system frequency.

In the dynamic responses of the network frequency, the PMSG' active power P_g, G_1's active power output P_{G1}, and G_2's active power output P_{G2} are compared for different control methods and different virtual inertia coefficients λ.

B. Comparison With Supplementary Derivative Control During Load Increase

To further illustrate the advantages of the proposed VIC scheme on inertia support and system damping, experimental results are

compared for the three cases: 1) *Case A*: without inertia control; 2) *Case B*: with the supplementary derivative control; and 3) *Case C*: with the proposed OPPT control.

During the tests, L1 was increased from 5.2 to 6.2 kW and the results for the three cases are shown in Figure. the change rate are reduced when inertia control is applied in Case B and Case C. Furthermore, Case C with the proposed VIC has the smallest frequency drop and smoothest recovery. This can be explained by observing the wind turbine power outputs between the proposed OPPT controller and the supplementary controller.

C. Comparison With Supplementary Derivative Control on Power Oscillation Damping After Short Circuit Fault:

In order to compare the effects of the OPPT control and the supplementary derivative control on power system oscillation damping, a 0.1-s three-phase short-circuit fault at Bus B2 was applied. The initial wind speed was 8 m/s and λ was set to an intermediate value of 7. In Fig., the ac voltage, the dc-link voltage of the PMSG's converters, the wind turbines' active power, and the active power of G1 are compared under the three same cases illustrated in the previous section. The severity of the three-phase short-circuit fault can be seen from the ac voltage waveforms shown in Fig.. For case A shown in Fig. when the short-circuit fault happens, the grid-side converter goes into current limit and its active power export to the grid is reduced. Since the generator-side converter controls the dc-link voltage, it automatically reduces power output from the PMSG and consequently the dc-link voltage remains stable with only less than 5% increase. During the fault period, the surplus mechanical power in the wind turbine is stored as kinetic energy in the wind turbines' rotating masses. However, the power oscillation in this weak network wind turbine makes no contribution to system damping under this basic control scheme.
As shown in Fig. for Case B, the fast active power response from the wind turbine to the network frequency variation is generated by the supplementary derivative controller.

1. Dynamic response of the network during suddenload increase:

1.1.Simulation results of without VIC

Frequency:

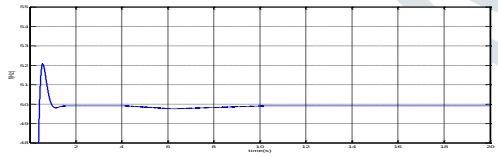

Fig.1.simulation of Time and frequency waveform

Active power (P_g):

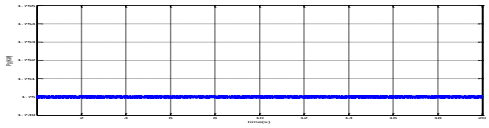

Fig.2.simulation of Time and active power waveform

G_1's active power output P_{G1}:

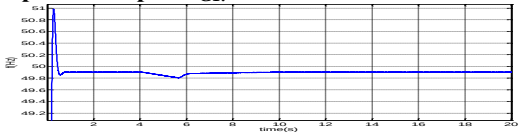

Fig.3.simulation of Time and G_1's active power output P_{G1} waveform.

G_2's active power output P_{G2}:

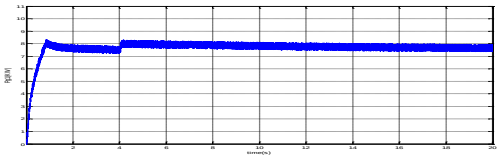

Fig.4.simulation of Time and G_2's active power output P_{G2} waveform

1.2.Simulation results of with VIC(λ=1):

Frequency:

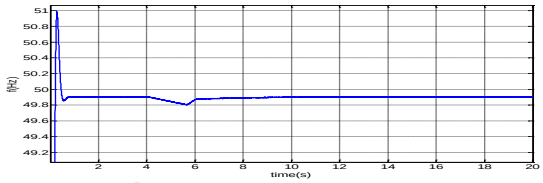

Fig.5.simulation of Time and frequency waveform.

G_1's active power output P_{G1}:

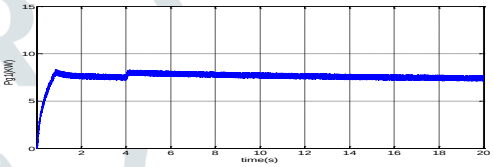

Fig.6.simulation of Time and active power waveform

G_2's active power output P_{G2}:

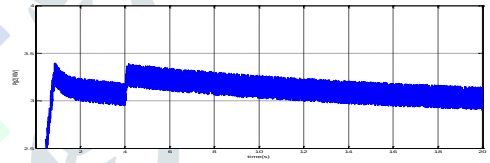

Fig.7.simulation of Time and G_1's active power output P_{G1} waveform

1.3.Simulation results of with VIC(λ=9):

Frequency:

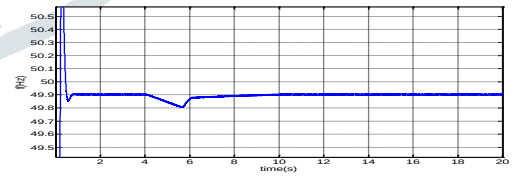

Fig.8.simulation of Time and frequency waveform

G_1's active power output P_{G1}:

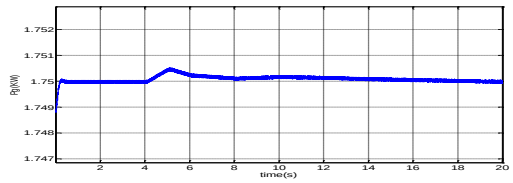

Fig.9.simulation of Time and G_1's active power output P_{G1} waveform

G_2's active power output P_{G2}:

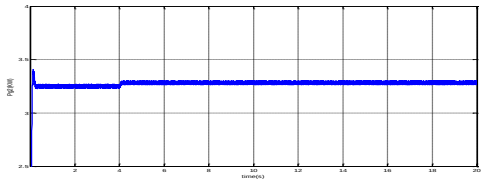

Fig.10.simulation of Time and G_2's active power output P_{G2} waveform

Simulation results of with VIC(λ=9):

Frequency:

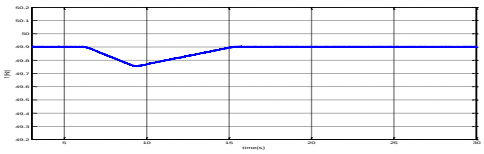

Fig.11.simulation of Time and frequency waveform

G_1's active power output P_{G1}:

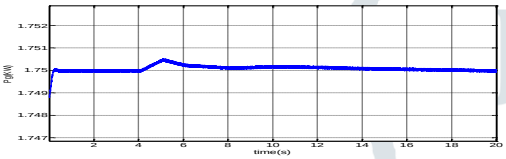

Fig.12.simulation of Time and G_1's active power output P_{G1} waveform

G_2's active power output P_{G2}:

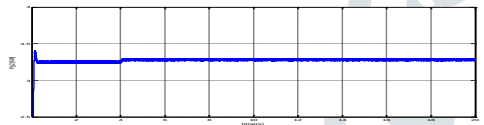

Fig.13.simulation of Time and G_2's active power output P_{G2} waveform

2.comparison of inertia response during sudden load increase:

Case A: Frequency:

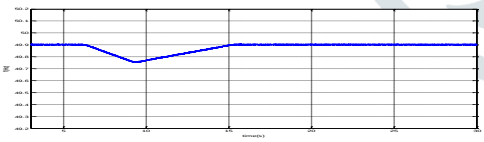

Fig.14.simulation of Time and frequency waveform.

G's active power output P_G:

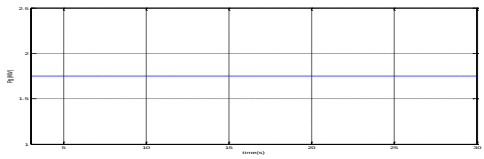

Fig.15.simulation of Time and G_1's active power output P_{G1} waveform

Case B: Frequency:

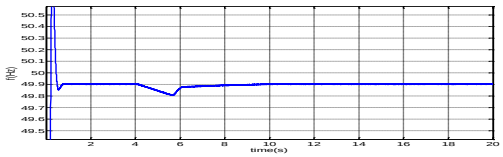

Fig.16.simulation of Time and frequency waveform

G's active power output P_G:

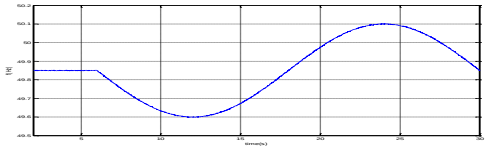

Fig.17.simulation of Time and G's active power output P_G waveform

Case C:

Frequency:

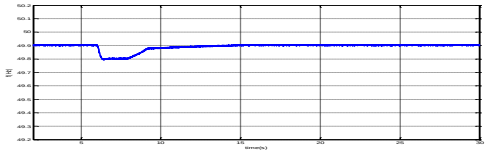

Fig.18.simulation of Time and frequency waveform

G's active power output P_G:

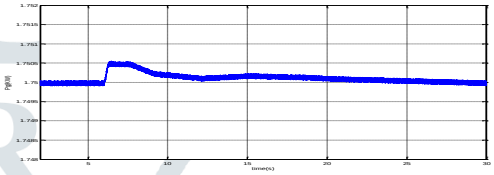

Fig.19.simulation of Time and G's active power output P_G waveform

3.Dynamic responses of the network after short-circuit fault :

AC Voltage:

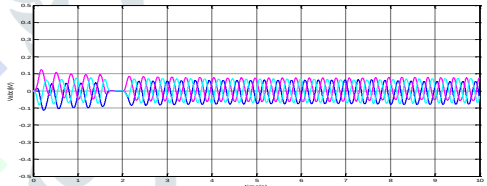

Fig.20.simulation of Time and voltage waveform

Case A: Voltage V_{dc}:

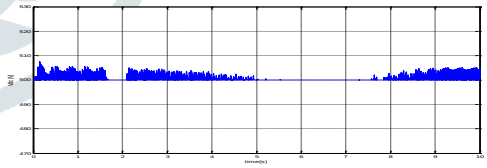

Fig.21.simulation of Time and voltage waveform

Active power P_G:

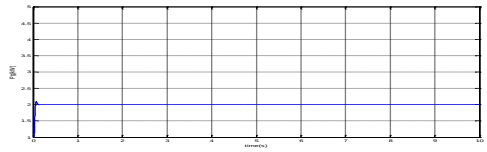

Fig.22.simulation of Time and G's active power output P_G waveform

Active power P_{G1}:

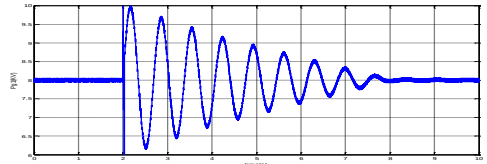

Fig.23.simulation of Time and G_1's active power output P_{G1} waveform

Case B:
Voltage:

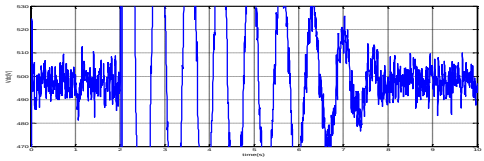

Fig.24.simulation of Time and voltage waveform

Active power P_G:

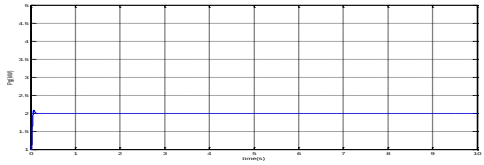

Fig.25.simulation of Time and G's active power output P_G waveform

Active power P_{G1}:

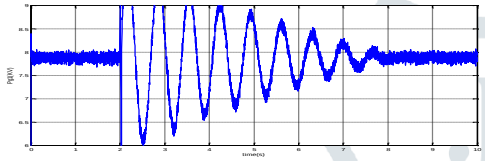

Fig.26.simulation of Time and G_1's active power output P_{G1} waveform

Case C:
DC Voltage:

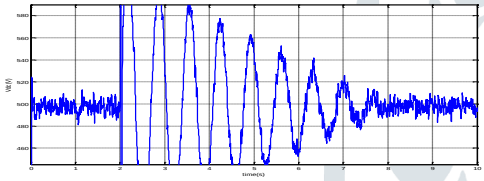

Fig.27.simulation of Time and voltage waveform

Active power P_G:

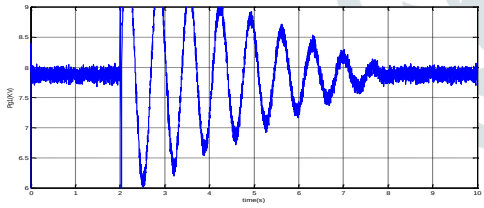

Fig.28.simulation of Time and G's active power output P_G waveform

4.Simulation results of sudden load change:
without VIC:
Frequency:

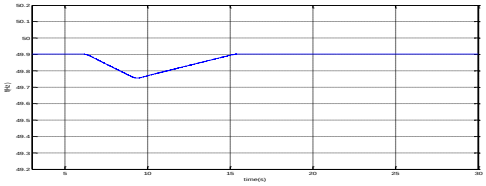

Fig.29.simulation of Time and frequency waveform

Active power P_G:

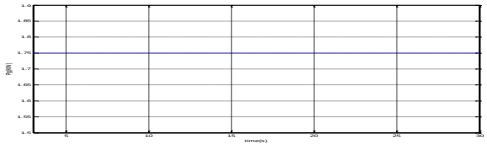

Fig.30.simulation of Time and G's active power output P_G waveform

With VIC(λ=1):
Frequency:

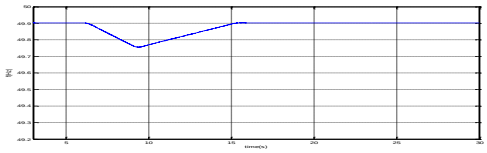

Fig.31.simulation of Time and frequency waveform

Active power P_G:

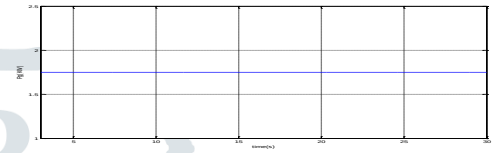

Fig.32.simulation of Time and G's active power output P_G waveform

with VIC(λ=9):
Frequency:

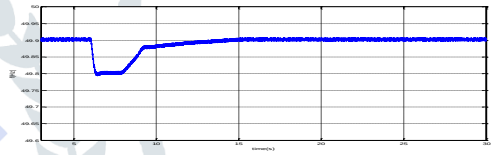

Fig.33.simulation of Time and frequency waveform

Active power P_G:

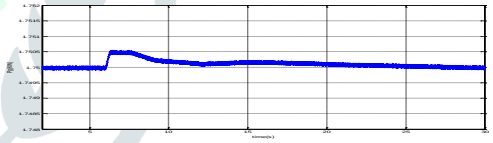

Fig.34.simulation of Time and G's active power output P_G waveform

5. Dynamic responses of network after short circuit fault:
AC Voltages:

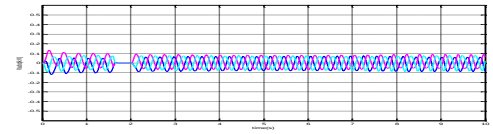

Fig.35.simulation of Time and voltage waveform

Case A : Voltage:

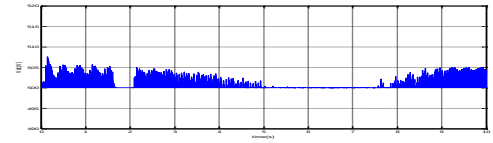

Fig.36.simulation of Time and voltage waveform

Active power P_G:

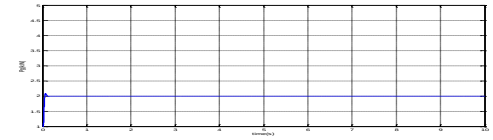

Fig.37.simulation of Time and G's active power output P_G waveform

Active power P_{G1}:

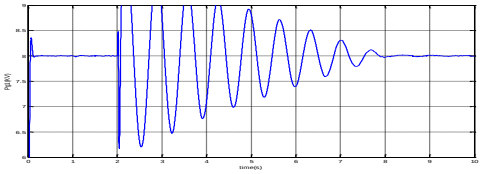

Fig.38.simulation of Time and G_1's active power output P_{G1} waveform

Case B:

Voltage:

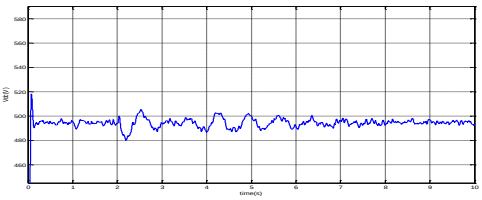

Fig.39.simulation of Time and voltage waveform

Active power P_G:

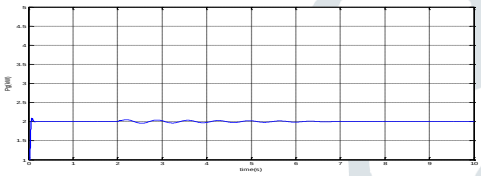

Fig.40.simulation of Time and G's active power output P_G waveform

Active power P_{G1}:

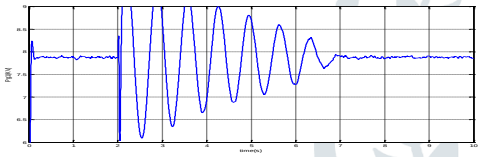

Fig.41.simulation of Time and G_1's active power output P_{G1} waveform

Case C: Voltage :

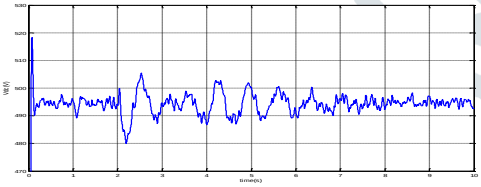

Fig.42.simulation of Time and voltage waveform

Active power P_G:

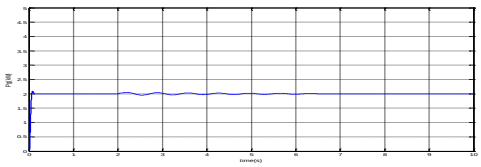

Fig.43.simulation of Time and G's active power output P_G waveform

Active power P_{G1}:

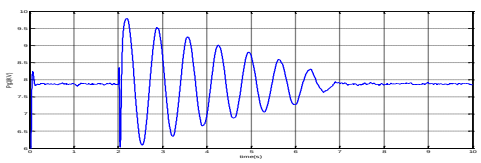

Fig.44.simulation of Time and G_1's active power output P_{G1} waveform

IX.CONCLUSION

The fuzzy logic controller(FLC) has been employed for power oscillation damping of PMSG and analysis of results of the performance of a fuzzy logic controller is presented. The simulation of the complete drive system is described in this paper. Effectiveness of drive is established by performance prediction over a wide range of operating conditions. A performance comparison between the fuzzy logic controller and the conventional PI controller has been carried out by simulation runs confirming the validity and superiority of the fuzzy logic controller to be adjusted such that manual tuning time of the classical controller is significantly reduced. The performance of control of PMSG with virtual inertia control method has been developed to be reference of PI controller , FLC controller verified with conventional PI controller using simulation. Fuzzy logic controller improved the performance of control of PMSG with VIC control drive of the fuzzy logic controller.

X.REFERENCES

[1] N. Millerand P.E. Marken, "Facts on grid friendly wind plants, "in Proc. IEEE Power Energy Soc. Gen. Meeting, 2010, pp.1–7

[2] M. Cardinal and N. Miller, "Grid friendly wind plant controls: Wind control-field test results," in Proc. Amer. Wind Energy Conf., 2006, pp.1–8.

[3] J.Morren, S. de Haan, W. Kling, and J. Ferreira, "Wind turbinesemulatinginertiaandsupportingprimaryfrequencycontrol,"IEEETrans.Power Syst., vol. 21, no. 1, pp. 433–434, Feb.2006.

[4] J.EkanayakeandN.Jenkins,"Comparisonoftheresponseofdoublyfed and fixed-speed induction generator wind turbines to changes in network frequency," IEEE Trans. Energy Convers., vol. 19, no. 4, pp. 800–802, Dec.2004.

[5] L.Holdsworth, J. B. Ekanayake, and N. Jenkins, "Power system fre- quency response from fixed speed and doubly fed induction generator- based wind turbines," Wind Energy, vol. 7, no. 1, pp. 21–35, Mar. 2004.

[6] A.Mullane and M. O'Malley, "The inertial response of induction- machine-based wind turbines," IEEE Trans. Power Syst., vol. 20, no. 3, pp. 1496–1503, Aug.2005.

[7] J.G.Slootweg and W. L. Kling, "The impact of large scale wind power generation on power system oscillations, "Electr. Power Syst. Res., vol. 67, no. 1, pp. 9–20, Feb.2011.

[8] G. Tsourakis, B. M. Nomikos, and C. D. Vournas, "Contribution of doubly fed wind generators to oscillation damping," IEEE Trans. Energy Converters., vol. 24, no. 3, pp. 783–791, Sep.2009.

[9] Z. S. Zhang, Y. Z. Sun, and J. Lin, "Coordinated frequency regulation by doubly fed induction generator-based wind power plants, "IET Renew. Power Gener., vol. 6, no. 1, pp. 38–47, Jan.2012.

[10] G.Ramtharan,J.B.Ekanayake,andN.Jenkins,"Frequencysupportfrom doubly fed induction generator wind turbines, "IET Renew. Power Gener., vol. 1, no. 1, pp. 3–9, Mar.2007.